JOURNAL OF GEOPHYSICAL RESEARCH, VOL. 88, NO. C3, PAGES 1800–1808, FEBRUARY 28, 1983

Scylla and Charybdis Observed From Space

WERNER ALPERS

Institut für Geophysik, Universität Hamburg and Max-Planck-Institut für Meteorologie, Hamburg, Federal Republic of Germany

ETTORE SALUSTI

INFN, Istituto di Fisica Guglielmo Marconi, Università di Roma, Rome, Italy

Scylla and Charybdis are, in Greek mythology, two immortal and irresistible monsters who beset the narrow waters separating the Italian peninsula from Sicily. They give poetic expressions to exceptional oceanographic features encountered in the Strait of Messina. Recently, the SEASAT satellite has added new information on the oceanography of this strait. For the first time, experimental evidence is presented that internal waves are generated in the Strait of Messina. The generation mechanism is linked to tidal currents washing over the shallow sill within the strait. The experimental data originate from a synthetic aperture radar (SAR) image obtained from the SEASAT satellite on Sept. 15, 1978, and from subsequent in situ measurements carried out from the Italian research vessel *Bannock* in Nov. 1980. The circular wave pattern visible on the SEASAT SAR image is interpreted in terms of internal solitons. Furthermore, the SEASAT SAR image also reveals 'tagli,' special types of tidal bores, encountered in the Strait of Messina.

1. INTRODUCTION

The Strait of Messina separating the Italian peninsula from the island of Sicily has been known since ancient times as an area of strong currents and vortices. To our knowledge, the first documented hypothesis about the origin of the violent currents in the Strait of Messina was from Homer (around 800 B.C.), who thought that they are caused by two monsters, Scylla and Charybdis (Homer, *Odyssey*, 12th song, line 80–114). Later, Aristotle (384–322 B.C.) tried to explain the oceanographic phenomena in this strait by hollows in the seafloor and by an interaction of two opposing wind generated currents (Aristotle, *Problemata Physica*, chap. 23).

But more than 2000 years elapsed before scientific oceanographic measurements were carried out in this area. The French vice-consul in Messina, Ribaud, in A.D. 1824 already gave a fairly detailed description of the current conditions in the Strait of Messina [see *Vercelli*, 1925], but oceanographic measurements were not carried out before A.D. 1922. In 1922 and 1923, during two cruises with the research vessel *Marsigli*, the Italian oceanographer Vercelli made the first extensive oceanographical survey of this area. The oceanographic data Vercelli collected are still considered to be the most detailed and systematic data from the Strait of Messina up till now.

The analysis and theoretical interpretation of Vercelli's data has been performed by *Vercelli* [1925], *Vercelli and Picotti* [1925], and *Defant* [1940, 1960], and is still performed [*Brandolini et al.*, 1980; *Hopkins* et al., 1982]. It can be concluded from Vercelli's measurements that the current distribution within the Strait of Messina is largely a result of tidal action. At first glance this seems to be surprising, since the amplitudes of the tides are known to be very low in the Mediterranean Sea (of the order of 10 cm). But in the Strait of Messina a large gradient of the tidal amplitude is encountered because the tides in the basin north of the strait (Tyrrhenian Sea) and south of the strait (Ionian Sea) are out of phase by almost 180 degrees.

Since it is well known that internal wave trains are generated by tidal action at the Strait of Gibraltar [*Frassetto*, 1964; *Ziegenbein*, 1969; *Lacombe*, 1971], and the Strait of Georgia, British Columbia [*Gargett*, 1976], one might expect that the same occurs at the Strait of Messina. But though the straits of Gibraltar and Messina are in many respects very similar, there are also pronounced differences. For example, the depth of the sill is approximately 300 m in the Strait of Gibraltar, while it is 100 m in the Strait of Messina. The flow on the sill in the Strait of Gibraltar is strictly baroclinic, while in the Strait of Messina it is largely barotropic. The Strait of Georgia, on the other hand, differs from these two European straits, e.g., by the depth of the pycnocline, which is in the Strait of Georgia only a few meters. There, the strong density stratification is due to fresh water inflow from a river.

In this paper we present for the first time experimental evidence that internal waves are generated at the Strait of Messina. Their existence was first inferred from a synthetic aperture radar (SAR) image obtained from the SEASAT satellite at an altitude of 800 km on Sept. 15, 1978. (A detailed description of the SEASAT synthetic aperture radar can be found in *Jordan* [1980]). Subsequent in situ measurements carried out from the Italian research vessel *Bannock* in Nov. 1980 [*Abbate et al.*, 1982] support the conclusion drawn from the satellite image.

Furthermore, the SEASAT image also reveals 'tagli' (tidal bores) in the Strait of Messina. To our knowledge, this is the first time that tidal bores have been identified on a SAR image.

2. DESCRIPTION OF THE SEASAT-SAR IMAGE

SEASAT SAR data over Europe have been received by the ESA (European Space Agency) station at Oakhanger in England, which was operated by the Royal Aircraft Establishment. Only 53 passes over Europe with 272 min worth of data have been recorded, among them five passes over the

Paper number 2C1364.
0148-0227/83/002C-1364$05.00

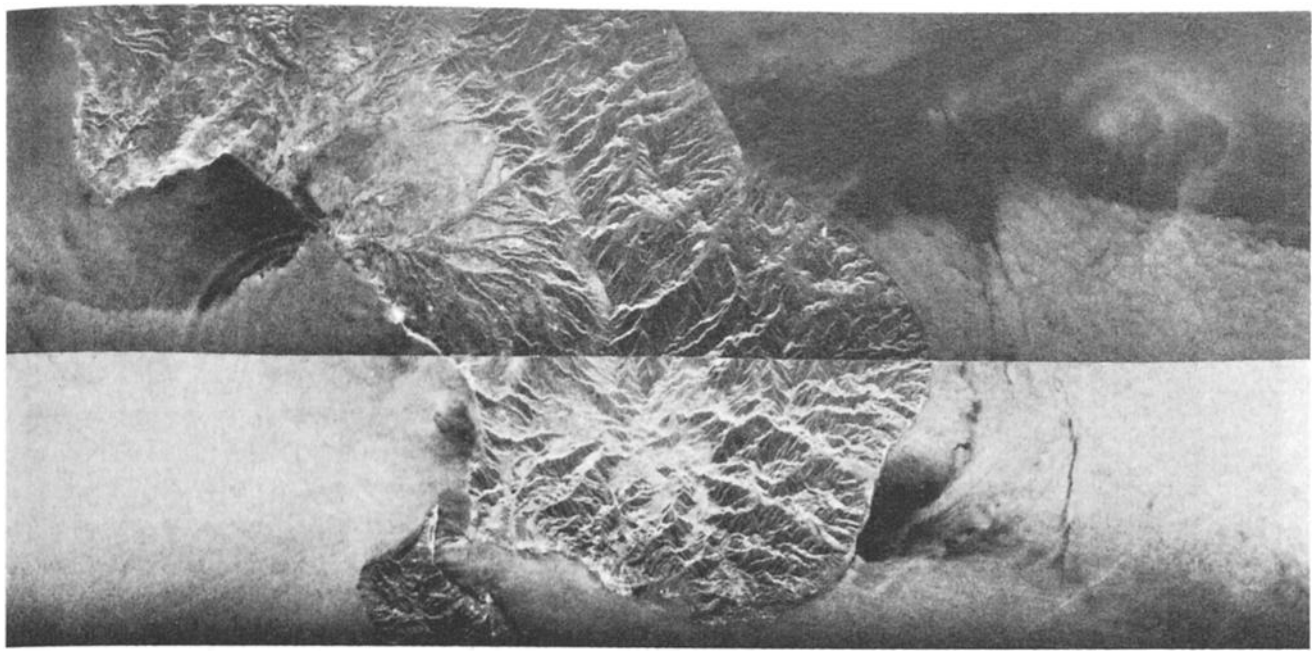

Fig. 1. Optically processed SAR image from SEASAT orbit 1149 (Sept. 15, 1978, 0817 GMT) showing the southern part of the Italian peninsula (Calabria), Sicily, the Strait of Messina, and part of the Tyrrhenian Sea (Golfo di Gioia).

Mediterranean and only one (orbit 1149) over the Strait of Messina on Sept. 15, 1978, at approximately 0817 GMT. All European data were first survey processed on an optical processor at the Environmental Research Institute of Michigan (ERIM). The spatial resolution is approximately 25 m × 25 m (4 looks). Subsequently, part of the data was precision processed in Germany at the 'Deutsche Forschungs- und Versuchsanstalt für Luft- und Raumfahrt' (DFVLR) on the MDA (MacDonald Dettwiler and Associates) digital SEASAT SAR processor. The spatial resolution is again 25 m × 25 m (4 looks), and the image area is 40 km × 40 km.

Figure 1 shows an optically processed image from SEASAT orbit 1149. One recognizes in the center the southern part of Italy (Calabria) and on the bottom (to the left) the northeast corner of Sicily. Both land areas are separated by the Strait of Messina. Figure 2 shows a digitally processed image of a 40 km × 40 km subsection of the same area with the frame center located at 38°20′46″N and 15°49′56″E. Figure 3 is a schematic map of the imaged scene in which the most important features visible on the SAR image are marked.

The most pronounced oceanic features visible on both images are the three rings in the Tyrrhenian Sea (Golfo di Gioia), approximately 30 km north of the Strait of Messina. They are particularly well visible in the dark region, which is a sea area of low radar backscattering. The rings extend also into the bright area, as can be seen on the survey processed image (Figure 1). The spacing of the rings varies between 1800 m and 700 m; it is largest at the front (north) and decreases to the rear (south). The spacing of the rings is narrower near the coast (east) than further out to the sea (west). In the next section we present evidence that these rings are surface manifestations of internal wave trains generated in the strait.

Furthermore, in the coastal region near Palmi another wave-type pattern is visible. It is much less pronounced, consists of waves with a wavelength of approximately 300 m, and seems to have its origin in the shallow sea area near Palmi.

Another feature discernible on both images are the two bright bands connecting Punta Pezzo in Calabria with the Sicilian coast. To the northeast of these two bands, other less bright bands are visible which are interdispersed by dark regions. They are bands or increased surface roughness and are interpreted as surface manifestations of 'tagli' (Italian: cuts or profiles). Tagli are a special kind of tidal bores [*Defant*, 1960] encountered in the Strait of Messina. They are probably associated with a hydrolic jump, but this has never been measured. Their position within the strait is mainly determined by lunar time. The tagli are also visible by the naked eye from a boat. The local fishermen regulate their embarkation time for fishing according to the passage of these tagli, since they mark boundaries of water masses of different biological quality. In the next section, we shall discuss in more detail what is known about the tagli from a physical point of view.

3. Oceanographic Conditions in the Strait of Messina

The Strait of Messina separates the Italian peninsula from the island of Sicily. It is a natural connection between the Tyrrhenian Sea in the northwest and the Ionian Sea in the southeast. The width of the strait at the narrowest point is approximately 4 km, and the average depth is 85 m. The sea bottom slopes gradually down approximately 1300 m toward the Ionian and 300–600 m toward the Tyrrhenian side. Thus, the strait constitutes a submarine barrier or sill for the water flowing through the channel (see Figure 4).

From the measurements Vercelli carried out in 1922 and 1923, the following picture concerning the current distribution in the Strait of Messina has emerged [*Vercelli*, 1925; *Brandolini et al.*, 1981]. At the narrowest point there is a

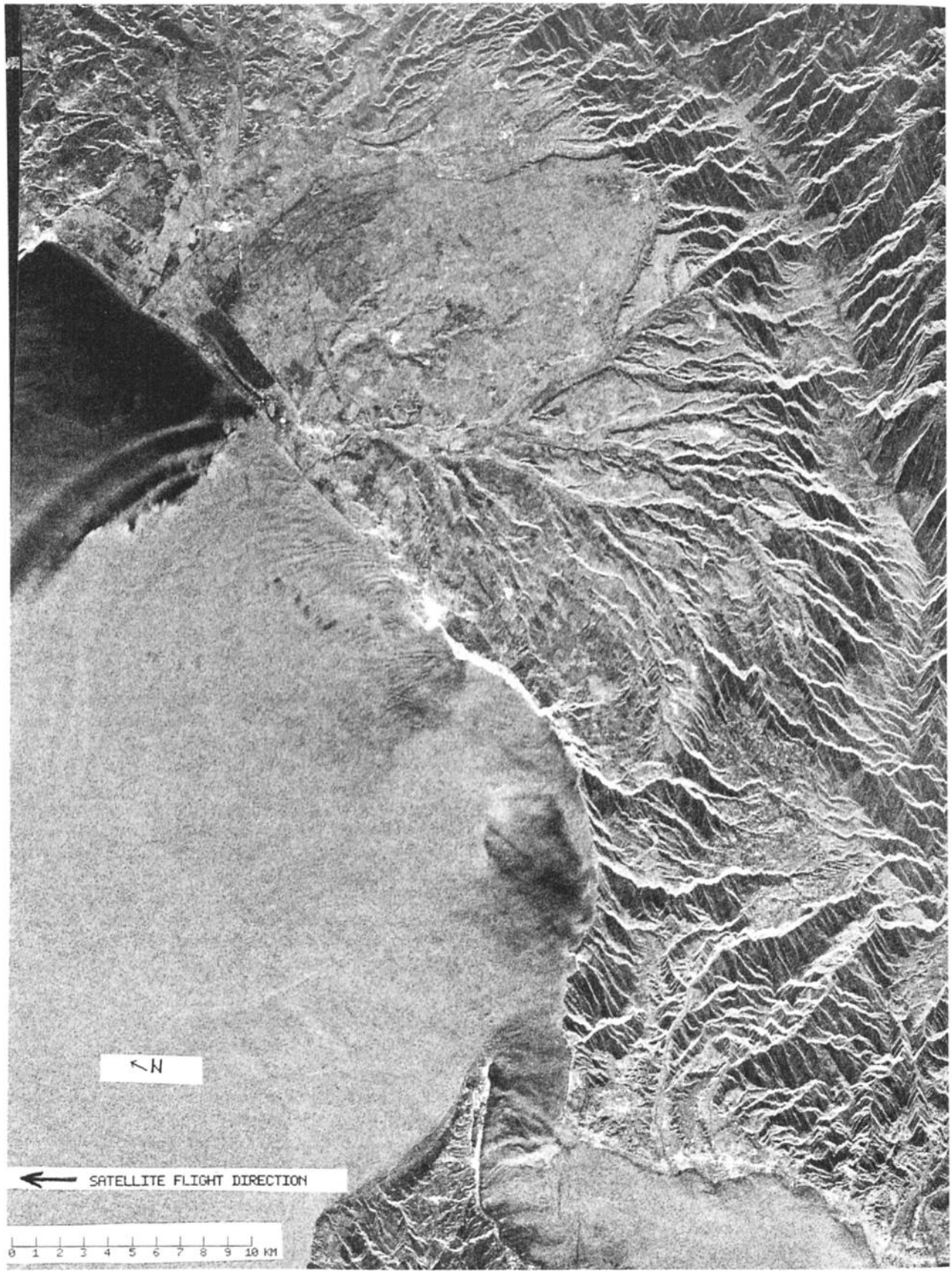

Fig. 2. Subsection of the area shown in Figure 1. This image was optically processed at the Deutsche Forschungs- und Versuchsanstalt fur Luft- und Raumfahrt (DFVLR) for the European Space Agency (ESA) (resolution: 25 m × 25 m, 4 looks).

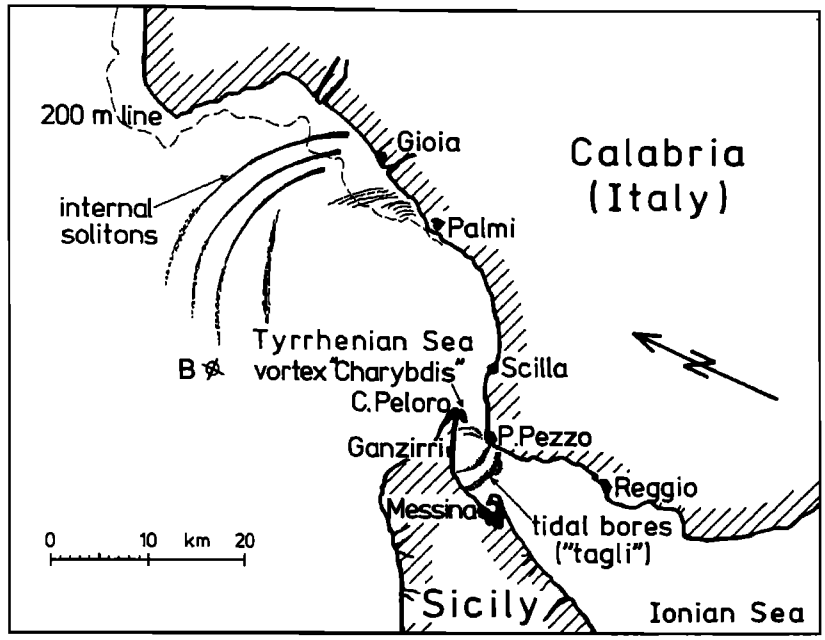

Fig. 3. Schematic map of the imaged scene. B is the position of the research vessel *Bannock*, where on Nov. 24 and 25, 1980, in situ measurements were carried out.

stationary surface current flowing in the southward direction and a bottom current flowing in the opposite direction.

Current reversal occurs at a depth of approximately 30 m. The time-averaged velocity of these currents is of the order of 10 cm s^{-1}. The Ionian water coming from the south is more saline and therefore heavier than the water coming from the Tyrrhenian Sea. The relative density difference is of the order of 10^{-3}.

Superimposed on these stationary currents are the tidal currents originating from the co-oscillation of the water masses of the strait with the tides of the adjacent seas. The tides are almost in phase opposition. This phase change occurs within a short distance of 3 km around Punta Pezzo-Ganzirri (narrowest point of the strait). Although the tidal amplitudes are relatively small (~10 cm), the sea surface slope can attain values of 1–2 cm/km, which leads to strong currents. During spring tide the current velocity can be as high as 2.8 m s^{-1}.

During maximum tidal flow from the Tyrrhenian Sea to the Ionian Sea (rema scendente) and from the Ionian Sea to the Tyrrhenian Sea (rema montante) only one type of water is encountered over the sill: lighter Tyrrhenian water in case of rema scendente and heavier Ionian water in case of rema montante. At these times the two-layer structure of the water column over the sill is absent. When the tide reverses, heavy water of the Ionian Sea rushes head on against the slowly receding lighter water of the Tyrrhenian Sea (start of rema montante), and lighter Tyrrhenian water glides over the heavier Ionian water (start of rema scendente). In both cases, tagli develop at the line of flow inversion. They propagate in the direction from the basin of low tide to the basin of high tide. The tagli resemble bores in estuaries. They manifest themselves on the surface by bands of increased surface roughness 'as if a strong wind were blowing' [*Vercelli*, 1925, chap. 5]. In these bands the water is very choppy. Usually two or three strong tagli develop, which propagate along the strait with a velocity of the order of 1–5 knots. They are not only encountered at lines of flow inversion but also at regions of strong flow convergence. Their position and shape depend primarily on lunar time and also on the day of the month and on the wind. The tagli are most pronounced around the line Punta Pezzo-Ganzirri. Based on his own point observations and on information given by the 'fishermen,' especially by Mr. Peppino Arena, fisherman at the Institute of Marine Biology at Messina, *Vercelli* [1925] has drawn figures showing the approximate positions of the tagli at different lunar hours. His description of the phenomenon is still the most detailed one up to now.

4. INTERPRETATION OF THE SEASAT-SAR IMAGE

Unfortunately, no in situ oceanographic measurements were carried out during the SEASAT overflight. Thus, the interpretation of the oceanic features visible on the SEASAT-SAR image can only be based on theoretical arguments

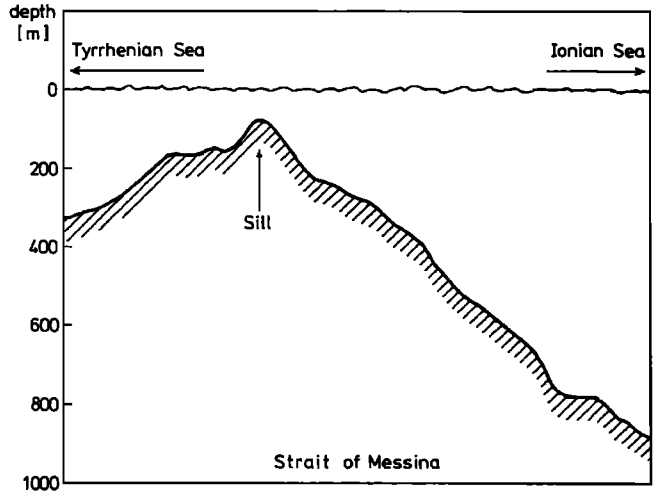

Fig. 4. Depth profile of the Strait of Messina.

and on estimates of the oceanographic parameters obtained from former and latter in situ measurements. As stated before, the best systematic former measurements are by Vercelli, and they are almost 60 years old. Motivated by this SEASAT image, in situ measurements were performed later with the aim of detecting internal wave trains generated at semi-diurnal tidal intervals in the Strait of Messina [*Abbate et al.*, 1982]. In the next section we report about these measurements, which support our interpretation of the SEASAT data.

The SEASAT image was taken on Sept. 15, 1978, approximately at 0817 GMT. According to the tide table of the Strait of Messina, still water occurred at 2330 GMT on Sept. 14, 1978, maximum current (between 2.5 and 3 knots) from the Ionian Sea into the Tyrrhenian Sea at 0223 GMT on Sept. 15, still water at 0454 GMT, and maximum current (between 5 and 5.5 knots) from the Tyrrhenian Sea into the Ionian Sea at 0807 GMT.

The above times coincide with a spring tide. The weather report from that day states the following wind conditions. 0600 GMT: island of Ustica (38°42′N, 13°11′E): Beaufort 3, NW (250 m above sea level); Capo Palinuro, Calabria (40°1′N, 15°17′E): calm (185 m above sea level); Messina, Sicily (38°12′N, 12°33′E): calm (51 m above sea level). 1200 GMT: Ustica: Beaufort 3, WNW; Capo Palinuro: Beaufort 3, WNW; Messina: Beaufort 2, N. From these weather reports we conclude that the wind conditions at sea level in the Golfo di Gioia (the area where the concentric rings are visible) on Sept. 15, 1978, at 0817 GMT are 2–3 m s^{-1} from NW to WNW, with probably lower winds (calm) near the Calabrian coast.

Nonlinear Internal Wave Train

We hypothesize that the circular pattern on the SEASAT image consisting of three rings is a nonlinear internal wave train or a packet of internal solitons generated at the Strait of Messina. Furthermore, we hypothesize that the internal solitons are generated when heavy Ionian water starts flowing from the south over the sill into the Tyrrhenian Sea (i.e., during tidal flow inversion from rema scendente to rema montante). This intrusion of heavy water depresses the thermocline on the Tyrrhenian side of the strait of Messina. Theory predicts that internal solutions may emerge from such an impulsive downward depression of the thermocline [*Gardner et al.*, 1967; *Osborne and Burch*, 1980]. Such a reverse in the tidal flow direction occurred at 2330 GMT on Sept. 14, 8 hours and 47 minutes before the SEASAT SAR image was taken.

Since the distance of the leading edge of the internal solution train is 33 km from the sill, we obtain for the propagation velocity

$$c = \frac{33 \text{ km}}{8 \text{ h } 47 \text{ min}} = 1.0 \text{ m s}^{-1} \tag{1}$$

We now compare this measured value with theoretical estimates. According to the theory of solitons as first described by *Korteweg and de Vries* [1895], the propagation speed of an internal soliton is given by [*Apel*, 1982]

$$c = c_0[1 + \alpha(\eta_0)] \tag{2}$$

where c_0 is the phase speed of a small amplitude internal wave and α a monotonically increasing function of wave amplitude η_0. According to *Apel* [1981], highly nonlinear internal waves (which he calls 'damped cnoidal' internal waves) can have speed increments α (η_0) of the order of 25%. Let h_1 and h_2 ($\gg h_1$) be the thickness, and ρ_1 and ρ_2 the density of the upper and lower layers of a stratified sea, respectively, then c_0 is given by

$$c_0 \approx \left(g \frac{\Delta\rho}{\rho} \frac{h_1}{1 + r} \right)^{1/2} \tag{3}$$

where g is the acceleration of gravity (9.81 m s^{-2}), $r = h_1/h_2$, and $\Delta\rho = \rho_2 - \rho_1$ the density difference between the two layers. An expression for α, valid for certain idealized situations, has been derived by *Osborne and Burch* [1980]

$$\alpha(\eta_0) = \frac{1}{2} \frac{1 - r}{h_1} \eta_0 \tag{4}$$

Since we have no measurements of these parameters during the SEASAT overflight, we insert the values obtained during the *Bannock* cruise in Nov. 1980 into the above equations (see section 5). We obtain with

$$h_1 = 40 \text{ m}, \; h_2 = 450 \text{ m}, \; \Delta\rho/\rho = 1.3 \times 10^{-3}, \text{ and } \eta_0 = 15 \text{ m},$$

$$c_0 = 0.68 \text{ m s}^{-1}$$

$$\alpha = 0.17 \tag{5}$$

$$c = 0.80 \text{ m s}^{-1}$$

This value of c is smaller than 1.0 m s^{-1}, which is the value inferred from the SEASAT image. But this is not an inconsistancy in view of the uncertainties in all of the estimates involved. Possible explanations for this difference are (1) the density stratification was stronger in Sept. 1978 than in Nov. 1980; (2) the propagation of the internal solitons took place in a moving medium (in summer often a mean current in a northeastward direction of the order of 0.1 m s^{-1} along the coast is encountered); (3) the speed increment due to the nonlinearity is larger than 0.12 m s^{-1} (if an upper limit of 25% is assumed, we obtain $c \leq 0.93$ m s^{-1}).

The three rings visible on the SEASAT SAR image are not exactly concentric, and their focus is not located exactly at the Tyrrhenian mouth of the Strait of Messina but at approximately 10 km east of this point. The reason could be the sloping bottom topography near the coast and/or a current flowing in the eastward direction (see above).

The wave-like pattern near Palmi (see also Figure 3) are probably secondary internal wave trains generated by the interaction of an internal solutions coming from the Strait of Messina with the shallow bottom topography near the coast (L. H. Larson, private communication, 1980).

Tagli (Tidal Bores) and Turbulences

At the time of the SEASAT overflight, there was maximum flow on the sill in the direction Tyrrhenian Sea-Ionian Sea (rema scendente). The position of the tagli on the SEASAT SAR image compares well with the position of the tagli which Vercelli reported from April 28, 1923, 1900 local time [*Vercelli*, 1925, Figure 50]. At this time, also maximum flow was encountered on the sill in a southward direction. Figure 5 is a reproduction of Vercelli's drawing. The similarity between the SEASAT image and Vercelli's drawing is striking.

Another feature on the SEASAT image worth mentioning,

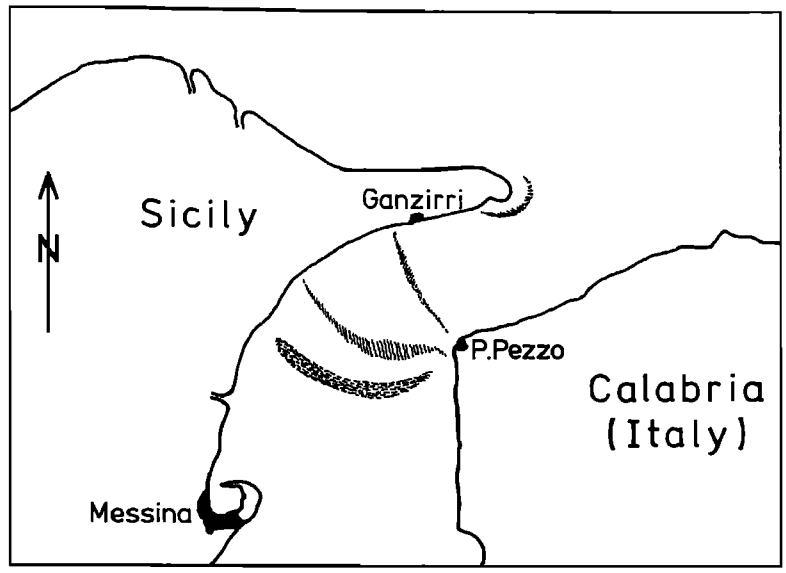

Fig. 5. Position of tagli (tidal bores) on April 28, 1923, 1400 local time as reported by *Vercelli* [1925]. At that time there was maximum flow into the southward direction (i.e., a similar flow condition was encountered as during the SEASAT overflight).

but not discussed further in this paper, is the dark area south of C. Peloro. This area is known since ancient times as the site of a strong vortex (the vortex 'Charybdis'). Also Vercelli reports that this area is always a region of strong turbulence. It is well known that turbulence decreases (or sometimes even wipes out) the short-scale ocean surface roughness responsible for the radar backscattering. (This effect, e.g., can be observed in the turbulent water (wake) produced by the propeller of a ship.) Thus, turbulent ocean areas are regions of low (or zero) radar backscattering and appear dark on a radar image. This fact then provides the explanation why the vortex Charybdis is imaged by SEASAT SAR as a dark spot.

5. In Situ Measurements in November 1980

Inspired by the SEASAT-SAR image from Sept. 15, 1978, of the Golfo di Gioia, oceanographic in situ measurements were carried out in the sea area north of the Strait of Messina on Nov. 24 and 25, 1980, during the cruise 'Judith 80' of the Italian research vessel *Bannok* [*Viola et al.*, 1981; *Abbate et al.*, 1982]. Measurements were taken at station B (38°29'N, 15°34'E, approximately 15 miles north of the Strait of Messina (see Figure 3)). The measurements consisted of temperature and salinity measurements with a bathysonde (*Neil Brown* 2) lowered from the ship at depths of 43 and 45 m and some CTD casts.

Most of the time the temperature T shows only small variations of the order of $\Delta T \approx 0.2$°C. But large quasi periodic oscillations with $\Delta T \approx 2$°C occur at intervals corresponding to approximately the semi-diurnal tidal period. In Figure 6 and 7 we show two such measurements at a depth of 43 and 45 m, respectively, from Nov. 24 and 25, 1980. The period of the oscillations of event 1 (Figure 6) varies between 14 and 8 min with a tendency to decrease from front to rear. The wave train comprises eight periods and has a duration of approximately 2 hours. Event 2 (Figure 7) has a less periodic appearance than event 1. The maximum period is about 34 min, and total duration is approximately 2 hours. It seems that also higher harmonics are present in the time record.

The most relevant observation in this context is that event 2 starts approximately 11 1/2 hours later than event 1.

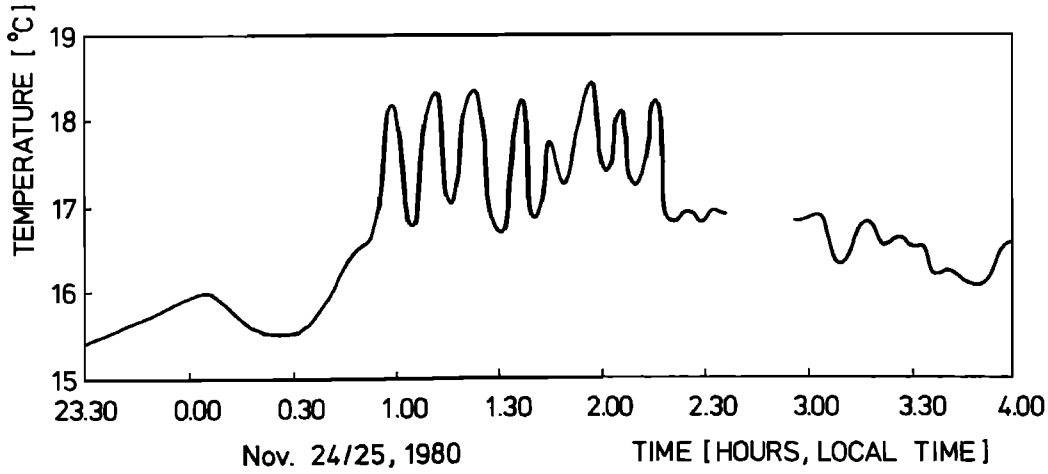

Fig. 6. Temperature profile measured on Nov. 24 and 25, 1980, at point B (see Figure 3) at a depth of 43 m.

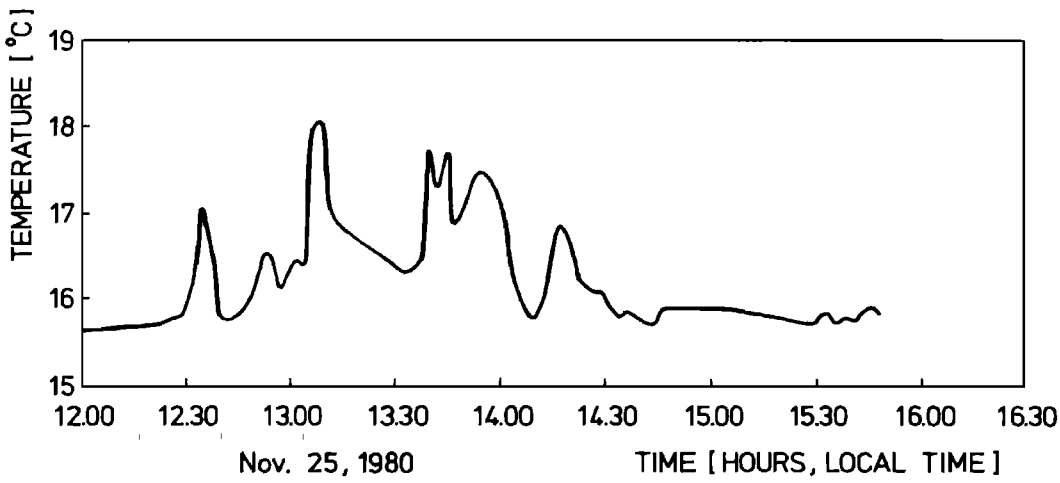

Fig. 7. Temperature profile measured on Nov. 25, 1980, at point B at a depth of 46 m.

According to the tide table of the Istituti Idrografico della Marina (Genova) the tidal current reversed sign from a southward to a northward direction on Nov. 24, 1980 at 1538 (local time) and on Nov. 25 at 0301. The time interval between these two current reversals is 11 h 22 min, which compares well the 11 1/2 h time lag between the arrival of internal wave trains at station B, and thus supports the hypothesis that the internal waves are generated by the tide at the sill. Under the assumption that the internal solitons are generated around slack water at the above given times, the travel time can be computed. We obtain for event 1 $T = 9$ h 25 min, and for event 2 $T = 9$ h 30 min. Since the distance between the observation point B and the sill is approximately 28 km, we obtain for both events

$$c \approx 0.82 \text{ m s}^{-1} \tag{6}$$

This value agrees quite well with the propagation velocity $c = 0.80$ m s^{-1} computed from equation (2) in section 4. The form of the two internal wave trains differ considerably. One possible explanation for this is that the details of the internal wave generation at the sill change from one semidiurnal cycle to the other. This is evidenced by the fact that the maximum flow at C. Peloro into the Tyrrhenian Sea was 0.9 m s^{-1} at 1755 (local time) on Nov. 24, and 2.1 m s^{-1} at 0612 on Nov. 25, which implies quite a difference in the strength of the flow inversion for event 1 and 2.

Another consistency check regarding the interpretation of the circular striation pattern on the SAR image in terms of internal waves can be obtained by comparing the wavelengths λ of this pattern with the in situ measured wave periods T and the calculated propagation speed c. Inserting in the equation

$$\lambda = c \cdot T \tag{7}$$

$c = 0.8$ m s^{-1} and 8 min $\leq T \leq$ 34 min we obtain

$$384 \text{ m} \leq \lambda \leq 1732 \text{ m} \tag{8}$$

which is consistent with the measured values for λ.

6. SAR Imaging Mechanism of Internal Waves

Since the penetration depth of electromagnetic waves of wavelength 23.5 cm (this is the SEASAT-SAR wavelength) is only of the order of a centimeter in sea water, the detectability of internal waves by SEASAT-SAR can only be due to some kind of surface manifestation. Since the radar return is determined by the short-scale roughness of the sea surface or, more precisely, by the spectral energy density of the Bragg waves [see, e.g., *Wright*, 1968, 1978; *Valenzuela*, 1978; *Alpers et al.*, 1981] the internal waves can become detectable if they modulate the short-scale roughness [*Brown et al.*, 1975; *Elachi and Apel*, 1976]. If the radar is a real aperture radar, then this is the only way they can become imaged. However, a synthetic aperture radar also responds to target motions. In addition to the 'real' cross-section modulation, caused by changes in the small-scale roughness, there exists for SAR also an 'artificial' cross-section modulation caused by motion effects [*Larson et al.*, 1976; *Alpers and Rufenach*, 1979; *Alpers et al.*, 1981]. This is caused by concentration and spreading of apparent position of backscatter elements due to variations of radial target velocities in azimuthal (flight) direction.

In the following, the last imaging mechanism will not be discussed any further, since for the case considered here it is probably not the dominating modulation mechanism. We only mention here, that artificial cross-section modulation is not relevant for internal waves traveling in range or azimuthal direction. It is largest when they travel 45 degrees to the flight direction.

Real cross-section modulation can be achieved by (1) surface films (slicks) that accumulate in flow convergence areas [*Lafond*, 1962] and damp the ripple waves there, or by (2) hydrodynamic interaction of the ripple waves with the horizontal surface current associated with internal wave motion.

If the first imaging mechanism applies, then on a SAR image only dark streaks (areas of low backscattering) are visible on a uniform background. Surface films, even when they are monomolecular, damp short waves very strongly [*Hühnerfuss et al.*, 1978, 1981] and thus reduce the radar return accordingly. Such films are often encountered in the ocean, where they are produced by plankton or fish. This imaging mechanism clearly can be ruled out for the present image. But often internal wave patterns have this kind of appearence on SAR (also on SEASAT-SAR) images.

If the second imaging mechanism applies, then the surface manifestation of internal waves are streaks that consist of

sections (sub-streaks) that are brighter and darker than the surrounding background. This is due to the fact that the short waves are positively or negatively 'strained,' depending on whether they propagate in convergent or divergent surface flow sections. In the first case, the spectral energy density of the Bragg scattering waves is increased, while in the second case it is decreased. Such hydrodynamic interaction has been investigated by *Longuet-Higgins and Stewart* [1964], *Bretherton and Garrett* [1968], *Keller and Wright* [1975], *Garrett and Smith* [1976], *Hughes* [1978], *Hughes and Grant* [1978], *Alpers and Hasselmann* [1978], and *Phillips* [1981]. The leading edge of an internal wave train appears as bright streak on a radar image, since this is a region of flow convergence and therefore a region of enhanced surface roughness [*Osborne and Burch*, 1980]. This imaging mechanism seems to be applicable in our case.

However, present theories on the hydrodynamic interaction between short surface waves and internal waves seem not to predict such strong modulations as evident from SAR imagery. The strength of the hydrodynamic interaction as described by these theories depend on the gradient $(d/dx)U_x$, where U_x is the horizontal flow velocity in the direction of the considered short wave component. Applied to radar imaging, this means that the x direction is identical to the look direction of the antenna.

For linear internal waves, the strain rate is given by [*Phillips*, 1977]

$$\frac{d}{dx} U_x = S_0 e^{i(kx - \omega t)} \tag{9}$$

where

$$S_0 = -ik_x \left(\frac{\delta\rho}{\rho} \frac{gk}{1 + \coth kh_1} \right)^{1/2} \frac{\eta_0}{\sinh kh_1} \tag{10}$$

Here k, ω, and η_0 denote the wave number, frequency, and amplitude of the internal wave. The phase is such that the regions of maximum convergence are above the modes of the thermocline displacement. For $kh_1 \ll 1$ equation (10) reduces to

$$S_0 = -i \frac{k}{h_1} \left(g \frac{\delta\rho}{\rho} h_1 \right)^{1/2} \eta_0 \tag{11}$$

Inserting $h_1 = 40$ m, $\delta\rho/\rho = 1.3 \times 10^{-3}$, $\eta_0 = 15$ m, and $k = 2\pi/700$ m^{-1} in equation (11) yields $|S_0| = 2.4 \times 10^{-3}$ s^{-1}. If $k = 2\pi/1800$ m^{-1} is inserted, then $|S_0| = 9.3 \times 10^{-4}$ s^{-1}. This horizontal strain rate is at least 1 order of magnitude smaller than the strain rate typically associated with long surface waves. Therefore, the modulation of the small-scale surface roughness by linear internal waves, and thus the radar cross section modulation, should be at least 1 order of magnitude smaller than the modulation caused by long surface waves. In general, this is not observed.

However, for strongly nonlinear internal waves, the horizontal strain rate may attain values of the order of 10^{-2} s^{-1} in certain regions (especially in convergence zones) as has been pointed out by *Pinkel* [1979] and J. Apel (private communication, 1980). In this case, the above-mentioned modulation theories may be sufficient to describe the SAR imaging of internal waves even quantitatively. But though in general the simple hydrodynamic modulation theories seem not to be adequate to explain the observed large cross-section modulation by internal waves, they nevertheless predict certain qualitative aspects of the imaging. According to theory [*Alpers et al.*, 1981], hydrodynamic modulation is largest for internal waves traveling in range direction and smallest for internal waves traveling in azimuthal direction. This implies that range traveling internal waves are imaged best, and azimuthally waves worst (or not at all), which is confirmed by experimental data [*Gower*, 1980]. Theory predicts further that the above statements apply better for L band imagery than for X band imagery [*Alpers et al.*, 1981]. As a consequence, azimuthally traveling internal waves should be better visible on X band than on L band radar images. This seems also to be confirmed by experimental data [*Gower*, 1980].

Recently a nonlinear wave modulation theory has been proposed by *Mollo-Christensen* [1982] to account for the observed large cross-section modulation. He attributes the large response of the short-scale roughness to small variations in the surface current field to finite amplitude effects and to the development of instabilities.

With respect to the SEASAT-SAR image of the Strait of Messina, we observe in the dark area west of Gioia an exceptionally strong modulation pattern. Probably the dark area is occupied by water which differs, e.g., by temperature from the surrounding bright area. A region of flow convergence is probably encountered at the boundary, which could give rise to the exhanced brightness at the interface of these two water masses. Since in that area the wind speed is around threshold for ripple wave generation, regions of strong flow convergence are probably preferred areas for the generation of short-scale roughness. But it cannot be excluded that the ripples in these regions are generated by the current itself. (An indication that this might be the case is that the wind is blowing almost tangentially to the ring pattern.) Therefore, the relative wind velocity relevant for the generation of the Bragg waves does not vary over the internal wave field. Dark streaks that should follow the bright streaks and which are associated with regions of the flow divergence cannot be seen in the dark sea area because they are below detection threshold.

Note that the visibility of the internal wave pattern is much less in the bright area due to the increased roughness of the background.

7. Discussion and Summary

The existence of strong currents and vortices in the Strait of Messina is known since ancient times, and there have been many attempts by writers, philosophers, and scientists in the last 27 centuries to explain their generation. Though the Strait of Messina has probably given more impetus to the development of oceanography than any other sea area in the world, surprisingly few modern oceanographic measurements have been performed in this region. The most detailed measurements were carried out from a ship in 1922 and 1923 by the Italian oceanographer Vercelli. Though his measurements resulted in a fairly detailed description of the currents and tagli (tidal bores) in the Strait of Messina, he was not aware of internal wave phenomena and therefore did not identify them in his data. To our knowledge, the SEASAT SAR image is the first record in which internal solutions, generated by the action of the tide in the Strait of Messina and propagating into the Tyrrhenian Sea, have been identified.

Thus, satellite imagery has provided first evidence that the activities of Scylla and Charybdis are also perceptible in a sea area more than 30 km away from the strait. In situ measurements carried out from the Italian research vessel *Bannock* 2 years later have confirmed the results derived from the SEASAT image.

In addition, this SEASAT image has provided for the first time a synoptic view of shape and position of the tagli in the Strait of Messina. Former descriptions by Vercelli have been based on measurements at one point (the position of the research ship) and on visual observations by fishermen.

Acknowledgments. We thank A. Viola and the other members of the Judith 80 cruise for permitting us to use their data prior to publication, the European Space Agency for supplying the SEASAT images at no costs, and M. Lüdecke for preparing the drawings.

REFERENCES

Abbate, M., A. Griffa, S. Marullo, E. Paschini, R. Santoleri, and A. Viola, Preliminary observations of large amplitude tidal internal waves near the Strait of Messina, report, Istit. di Fisica G. Marconi, Univ. di Roma, Italy, March 10, 1982.

Alpers, W., and K. Hasselmann, The two-frequency microwave technique for measuring ocean surface wave spectra from an airplane or satellite, *Boundary Layer Meteorol., 13*, 215–230, 1978.

Alpers W. R., and C. L. Rufenach, The effect of orbital motions on synthetic aperture radar imagery of ocean waves, *IEEE Trans. Antennas Propagat., AP-27*, 685–690, 1979.

Alpers, W., D. B. Ross, and C. L. Rufenach, On the detectability of ocean surface waves by real and synthetic aperture radar, *J. Geophys. Res., 86*, 6481–6498, 1981.

Apel, J. R., Nonlinear features of internal waves as derived from the SEASAT imaging radar, in *Oceanography From Space*, edited by J. F. R. Gower, pp. 525–533, Plenum, New York.

Brandolini, M., L. Franzini, and E. Salusti, On the tides in the strait of Messina, *Nuovo Cimento, 3C*, 671–695, 1981.

Bretherton, F. P., and C. J. R. Garrett, Wavetrains in inhomogeneous moving media, *Proc. R. Soc. London, Ser. A, 302*, 529–554, 1968.

Brown, W. E., C. Elachi, and T. W. Thompson, Radar imaging of ocean surface patterns, *J. Geophys. Res., 81*, 2657, 1975.

Defant, A., Scilla e Cariddi, e le correnti di marea nello Stretto di Messina, *Geof. Pura Appl., 2*, 93, 1940.

Defant, A., *Physical Oceanography*, vol. 2, Pergamon, New York, 1960.

Elachi, C., and J. R. Apel, Internal wave observations made with an airborne synthetic aperture imaging radar, *Geophys. Res. Lett., 3*, 647, 1976.

Frassetto, R., Short period vertical displacements of the upper layer of the Strait of Gibraltar, *SACLANTCEN T. R. 30*, SACLANT ASW Res. Center, La Spezia, Italy, 1964.

Gardner, C. S., J. M. Greene, M. D. Kruskal, and R. M. Miura, Method of solving the Korteweg-de Vries equation, *Phys. Rev. Lett., 19*, 1095–1097, 1967.

Gargett, A. E., Generation of internal waves in the Strait of Georgia, British Columbia, *Deep Sea Res., 23*, 17–32, 1976.

Garrett, C., and J. Smith, On the Interaction between long and short surface waves, *J. Phys. Oceanogr., 6*, 925–930, 1976.

Hopkins, T., E. Salusti, and D. Settimi, Tidal currents and internal waves in the Strait of Messina, 1982 report, Univ. di Roma, Italy, 1982.

Hühnerfuss, H., W. Alpers, and W. L. Jones, Measurements at 13.9 GHz of the radar backscattering cross section of the North Sea covered with an artificial surface film, *Radio Sci., 13*, 979–983, 1978.

Hühnerfuss, H., W. Alpers, W. L. Jones, P. A. Lange, and K. Richter, The damping of ocean surface waves by a monomolecular film measured by wavestaffs and microwave radars, *J. Geophys. Res., 86*, 429–438, 1981.

Hughes, B. A., The effect of internal waves on surface wind waves, 2, Theoretical analysis, *J. Geophys. Res., 83*, 455–465, 1978.

Hughes, B. A., and H. L. Grant, The effect of internal waves on surface wind waves, 1, Experimental measurements, *J. Geophys. Res., 83*, 443–454, 1978.

Jordan, R. L., The SEASAT-A synthetic aperture radar system, *IEEE J. Oceanic Eng., OE-5*, 154–164, 1980.

Keller, W. C., and J. W. Wright, Microwave scattering and straining of wind generated waves, *Radio Sci., 10*, 139–147, 1975.

Korteweg, D. J., and G. de Vries, On the change of long waves advancing in a rectangular canal and a new type of long stationary waves, *Phil. Mag., 5*, 422, 1895.

Lacombe, H., Le détroit de Gibraltar; Oceanographie physique, Memoire explicatif de la carte géotechnique de Tanger, *Notes et Memo.*, Serv. Géol. du Maroc, 1971.

Lafond, E. C., Internal waves, *The Sea*, edited by M. N. Hill, vol. 1, part 1, pp. 731–751, Interscience, New York, 1962.

Larson, T. R., L. I. Moskowitz, and J. W. Wright, A note on SAR imagery of the ocean, *IEEE Trans. Antennas Propagat., AP-24*, 393–394, 1976.

Longuet-Higgins, M. S., and R. W. Stewart, Radiation stresses in water waves, a physical discussion with applications, *Deep Sea Res., 11*, 529–562, 1964.

Mollo-Christensen, E., Variable current as a cource of excitation of nonlinear wave modulations, submitted to *J. Geophys. Res.*, 1982.

Osborne, A. R., and T. L. Burch, Internal solitons in the Andaman Sea, *Science, 208*, 451–460, 1980.

Phillips, O. M., *The Dynamics of the Upper Ocean*, Cambridge University Press, New York, 1977.

Phillips, O. M., The structure of short gravity waves on the ocean surface, in *Spaceborne Synthetic Aperture Radar for Oceanography*, edited by R. C. Beal, P. S. DeLeonibus, and I. Katz, The Johns Hopkins University Press, Baltimore, Md., 1981.

Pinkel, R., Observation of strongly nonlinear internal motion in the open sea using a range-gated Doppler sonar, *J. Phys. Oceanogr., 9*, 675–686, 1979.

Valenzuela, G. R., Theories for the interaction of electromagnetic and ocean waves—A review, *Boundary Layer Meteorol., 13*, 61–85, 1978.

Vercelli, F., *Crociere per lo studio dei fenomeni nello Stretto di Messina (R. N. Marsigli, 1922–1923)*, vol. 1, *Il regime delle correnti e delle mare nello Stretto di Messina*, Commissione Internazionale del Mediterraneo, Venice, Italy, 1925.

Vercelli, F., and M. Picotti, *Crociere per lo studio dei fenomeni nello Stretto di Messina (R. N. Marsigli, 1922–1923)*, vol. 2, *Il regime chimico fisico delle acque nello Stretto di Messina*, Commissione Internazionale del Mediterraneo, Venice, Italy, 1925.

Viola, A., A. Griffy, S. Marullo, F. Mele, and R. Santorelli, Informazione preliminari sulla determinazione sperimentale della struttura dell'acqua profonda nei Mari Adriatico e Tirreno Meridionale, Campagna Judith, November 1980, report Istit. di Fisica G. Marconi, Univ. di Roma, Jan. 12, 1981.

Wright, J. W., A new model for sea clutter, *IEEE Trans. Antennas Propagat., AP-16*, 217–223, 1968.

Wright, J. W., Detection of ocean waves by microwave radar: The modulation of short gravity-capillary waves, *Boundary Layer Meteorol., 13*, 87–105, 1978.

Ziegenbein, J., Short internal waves in the Strait of Gibraltar, *Deep Sea Res., 16*, 479–487, 1969.

(Received December 2, 1981;
revised August 6, 1982;
accepted September 3, 1982.)